Eur Biophys J (1994) 23:51–58

European Biophysics Journal

Inactivation of voltage-dependent calcium current in an insulinoma cell line

Carla Marchetti [1], Carolina Amico [1], Daniela Podestà [2], Mauro Robello [2]

[1] Istituto di Cibernetica e Biofisica, Consiglio Nazionale delle Ricerche, Via Dodecanesco 33, I-16146 Genova, Italy
[2] Università degli Studi di Genova, Via Dodecanesco 33, I-16146 Genova, Italy

Received: 16 September 1993 / Accepted in revised form: 31 December 1993

Abstract. We have studied the mechanism of Ca current inactivation in the β-cell line HIT-T15 by conventional and perforated patch recording techniques, using two pulse voltage protocols and a combination of current and tail current measurements. In 5 mM Ca, from a holding potential of −80 mV, the maximum current showed a complex time course of inactivation: a relatively fast, double exponential inactivation ($\tau_{h1} \approx 12$ ms and $\tau_{h2} \approx 60$ ms) and a very slowly inactivating component ($\tau > 1$ s). The faster component (τ_{h1}) was due to the voltage-dependent inactivation of a low-threshold-activated (LVA), T-type current, which deactivates more slowly ($\tau \approx 3-5$ ms) than the other components ($\tau \approx 0.2-0.3$ ms). The intermediate component (τ_{h2}) was due to the Ca-dependent inactivation of a portion of the high-threshold-activated (HVA) current. A saturating dose of the dihydropyridine (DHP) nifedipine (10 μM) did not affect the LVA current, but inhibited by 68 ± 5% the transient, Ca-sensitive portion of the HVA current and by 33 ± 12% the long lasting component. We suggest that three components of the calcium current can be resolved in HIT cells and the main target of DHPs is a HVA current, which inactivates faster than the DHP-resistant HVA component and does so primarily through calcium influx.

Key words: β-cells – Perforated patch recording – Ca-dependent inactivation – Dihydropyridines

Introduction

Under physiological conditions, blood glucose levels are precisely controlled by the secretion of insulin from the β-cells of the pancreas. Insulin-secreting cells display a complex pattern of bursting electrical activity, which depends on blood glucose levels, is initiated by the closure of ATP-sensitive potassium channels, and is sustained by voltage-dependent calcium channels (reviewed in Ashcroft and Rorsman 1989). It has been proposed (Cook et al. 1991; Hopkins et al. 1991) that calcium channel inactivation plays a key role in the mechanism underlying both the active phase of a burst and the interburst interval and this hypothesis is partially supported by theoretical models (Keizer and Smolen 1991; Smolen and Keizer 1992).

Pancreatic β-cells have been shown to contain at least two types of calcium selective channels, distinguishable on the basis of their activation threshold, deactivation rate, and single channel properties (Satin and Cook 1988; Hiriart and Matteson 1988; Ashcroft et al. 1990; Sala and Matteson 1990; Sala et al. 1991, Parsey and Matteson 1993). In addition, the calcium current of β-cells revealed two distinct modes of inactivation: voltage-dependent and current-dependent inactivation. These two modes of inactivation have been described in rodent (Plant 1988; Hopkins et al. 1991), human (Kelly et al. 1991), and clonal β-cells (Satin and Cook 1989), but the current pattern present in the different kinds of β-cells also appeared to be dependent on the species (see review by Ashcroft and Rorsman 1989).

More recently, multiple types of high-threshold-activated pharmacologically distinct calcium channels have been reported in rat insulinoma and human pancreatic β-cells (Aicardi et al. 1991; Sher et al. 1992; Pollo et al. 1993). Similar types of high-voltage-activated current have been described in neuronal and endocrine cells. These currents do not fit with the original classification of an L-type slowly inactivating and an N-type, fast inactivating current (Fox et al. 1987); instead, they are characterized by different pharmacological sensitivity (Aosaki and Kasai 1989; Carbone and Swandulla 1989; Carbone et al. 1990; Swandulla et al. 1991), while their kinetic differences are less pronounced (Kasai and Neher 1992; Artalejo et al. 1992; Regan et al. 1991).

Dihydropyridine antagonists and agonists are among the most potent pharmacological tools to classify calcium channels: their effect allows one to define a type of high-

Correspondence to: C. Marchetti

voltage-activated calcium channel, usually referred to as L-type. Although the first reports led to the conclusion that the β-cells contained only DHP-sensitive calcium currents (Rorsman and Trube 1986; Plant 1988; Rorsman et al. 1988; Keahey et al. 1989), other studies reported weaker and incomplete sensitivity to DHPs (Satin and Cook 1988; Hopkins et al. 1991) and finally DHP-insensitive, ω-conotoxin-sensitive calcium channels have been clearly identified (Sher et al. 1991; Pollo et al. 1993). As already remarked, these channels are different from the DHP-insensitive N-type channels of Fox et al. (1987): they do not show fast inactivation and are similar to those reported in certain neurons (Kasai and Neher 1992).

In this study, we have used the Syrian hamster HIT-T15 clone, an insulinoma cell line which has retained the property of secreting insulin in response to glucose (Santerre et al. 1981), as a model for studying the properties, of the voltage-dependent calcium channels of β-cells (Satin and Cook 1988, 1989; Keahey et al. 1989; Hsu et al. 1991). Two pulse voltage protocols and a combination of current and tail current measurements allow us to dissect the various components of calcium current on the basis of their mechanism of inactivation and their dihydropyridine sensitivity. We show that the low-voltage-activated current inactivates through a purely voltage-dependent mechanism and is not affected by the DHP nifedipine, while high-voltage-activated currents show functional diversity both in inactivation properties and DHP sensitivity.

Methods

HIT-T15 β-cells were purchased from American Type Culture Collection at passage 59, maintained in Ham's F12 medium with 2.5% fetal calf serum and 10% dialyzed horse serum, and used between passage 60 and 70.

Calcium currents were measured with the patch-clamp technique in standard (Hamill et al. 1981) and perforated patch (Horn and Marty 1988) whole cell recording (WCR) configuration by an L/M EPC7 amplifier (List Electronic). Voltage stimulation, data acquisition and analysis were performed by an Atari Mega ST4 computer, equipped with a VR-ST interface (Instrutech Corporation, Minneola, NY, USA). Downward deflections represent inward (depolarizing) currents. Capitance transients were minimized by analog compensation and corrected using a computer generated P/4 protocol.

External and internal (pipette) solutions were designed to minimize the sodium and potassium conductances and maximize the current through calcium channels. The external solution contained (in mM): TEACl 130, $CaCl_2$ or $BaCl_2$ 5, $MgCl_2$ 1, 4-AP 4, Glucose 10, Hepes 5, with pH adjusted to 7.4 with Trizma base. In standard WCR, the pipette solution contained (in mM): CsCl 20, CsOH 110, aspartic acid 100, $MgCl_2$ 4, EGTA 5, Hepes 5 and ATP 3, pH = 7.4 with Trizma base.

The perforated patch configuration was obtained by supplementing the pipette solution with the polyene antibiotic nystatin (Sigma Chemical Co.). Nystatin was first dissolved in dimethylsulfoxide (DMSO, 50 mg/ml) and, immediately before the experiment, diluted in the pipette solution to a final concentration of 200 μg/ml with the aid of a brief sonication. In this case the pipette solution has the following composition (in mM): CsCl 55, Cs_2SO_4 70, $MgCl_2$ 7 and HEPES 10, pH = 7.3 with Trizma base. In order to facilitate the formation of gigaseals, the pipette tip (100–200 μm) was filled with nystatin-free solution, while the pipette bulk was backfilled with the nystatin containing solution (Horn and Marty 1988; Korn and Horn 1989). In control experiments, DMSO alone (0.2%) in the pipette did not cause any modification of the current transient, indicating that the solvent had no role in membrane perforation.

Calcium currents recorded in the nystatin perforated patch configuration were not different from those recorded in conventional WCR. The current amplitude increased as the series resistance decreased and reached values which were comparable, on average, with those of conventional recording. However, in the perforated patch configuration, it was more difficult to achieve a low (<10 MΩ) access resistance and the current reached a maximum in the potential range 0 to +10 mV, probably as a consequence of a higher series resistance error. Therefore, the tail current analysis gives only qualitative hints in this case.

In both conventional and perforated whole cell recording, the inward current was totally abolished by 1 mM $CdCl_2$. In the presence of this dose of cadmium, only a linear leak current persisted and this was adequately subtracted by the P/4 protocol up to +60 mV. At higher voltages, some cells displayed a cadmium insensitive outward current which deviated from linearity and therefore it was not adequately compensated by the P/4 paradigm. A similar "non-linear" leak has been reported previously (Satin and Cook 1988; Hiriart and Matteson 1988; Satin and Cook 1989) and was not investigated further, also because it occurred only at very high voltages.

Nifedipine (Sigma Chemical Co.) was prepared in 100% ethanol (10 mM) and diluted to the final concentration in the external bath. Control experiments showed that that solvent alone was completely ineffective at this dilution. ω-conotoxin, fraction GVIA (ω-cgtx), was obtained from Bachem (Bubendorf, Switzerland) and made up to the desired concentration in the external bath solution.

Results

In a sodium-free external solution containing 5 mM $CaCl_2$, depolarizing voltage steps delivered from a holding potential of −80 mV elicited an inward current which activated close to −40 mV and attained a maximum amplitude at +10 or +20 mV. As with previous studies in both endocrine and neuronal cells (Matteson and Armstrong 1986; Cota 1986; Hiriart and Matteson 1988; Swandulla and Armstrong 1988; Parsey and Matteson 1993), two components of the calcium current could be resolved on the basis of deactivation kinetics (Fig. 1). Tail currents recorded at −50 mV after brief ($\leq$10 ms) depo-

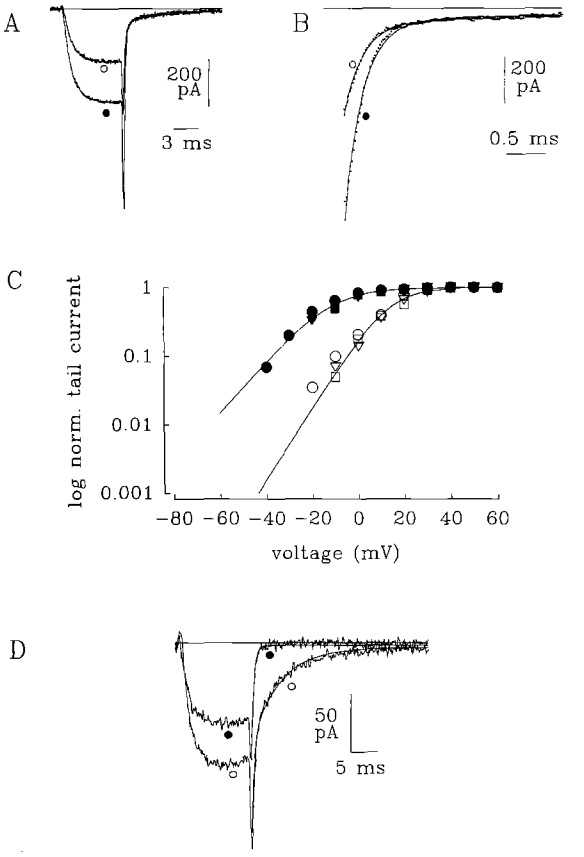

Fig. 1 A–D. Fast and slowly deactivating calcium currents in HIT cells. **A** Calcium current elicited by step depolarizations of 8 ms to +20 mV from a holding potential of −80 mV in 5 mM Ca (o) and 5 mM Ba (•). Repolarization potential was −50 mV. The sampling rate was 20 μs/point. Traces are averages of 10 consecutive recordings.

B Deactivation (tail) currents at −50 mV expanded from part A. Tail currents were approximated with the function:

$$I(t) = -A_1 \exp(-t/\tau_1) - A_2 \exp(-t/\tau_2).$$

The first 100 μs after onset of repolarization were blanked and exponential functions were extrapolated to zero. Best fit parameters were:

in 5 mM Ca, $A_1 = 504$ pA; $\tau_1 = 0.24$ ms; $A_2 = 62$ pA; $\tau_2 = 5.5$ ms;
in 5 mM Ba, $A_1 = 1095$ pA; $\tau_1 = 0.24$ ms; $A_2 = 51$ pA; $\tau_2 = 5.5$ ms.

C Activation curve for the two components of the calcium current in 5 mM external Ca. Tail currents after 8 ms steps to different voltages were approximated by a linear combination of two exponential functions as above and the relative amplitudes (A_1 and A_2) were normalized to the maximum value and plotted vs. voltage. Experimental points were fitted with the function:

$$I/I_{max} = 1/\{1 + \exp[-(V - V_{1/2})/K]\}$$

and the best fit parameters were:

SD current (*filled symbols*), $V_{1/2} = -13$ mV; $K = 8.3$ mV,
FD current (*empty symbols*), $V_{1/2} = 13$ mV; $K = 11$ mV.

Different symbols refers to three different cells.

D current traces obtained from a cell held at Vh = −80 mV (o) and Vh = −50 mV (•) and depolarized to +20 mV for 10 ms. Tail currents were approximated as above giving

for Vh = −80 mV, $A_1 = 360$ pA; $\tau_1 = 0.33$ ms; $A_2 = 92$ pA; $\tau_2 = 4.0$ ms;
for Vh = −50 mV, $A_1 = 300$ pA; $\tau_1 = 0.37$ ms; $A_2 = 0$ pA

larizations were approximated best by a double exponential function, with $\tau_1 \approx 0.3$ ms and $\tau_2 \approx 5$ ms. When calcium was replaced by equimolar barium, the fast component of the tail was increased by a factor of 2, while the slow component was virtually unchanged, and this indicates that the two channels have a different selectivity for divalent cations.

The voltage-dependent activation curve for the two components of the tail current was obtained by plotting the relative amplitude of the two exponential curves against the step potential (Fig. 1 C). The mid-point for activation (the voltage where half of the channels are open) was −13 mV for the slowly deactivating (SD) current and 13 mV for the rapidly deactivating (FD) current and these values are close to those of previous reports in rat β-cells (Hiriart and Matteson 1988; Sala et al. 1991; Parsey and Matteson 1993). From their activation properties, the two currents can be classified as low-voltage-activated (the SD current) and high-voltage-activated (the FD current).

These experiments also permit one to estimate the percentage of the SD current present in these cells. In 29 cells, 6 cells (20%) did not show any measurable slow component in the tail; in 13 cells (45%) the slowly deactivating current contributed ≤10% to the total current at +10 mV and in 10 cells (35%) the slow component contributed between 10 and 25%. The percentage of cells lacking the SD component increased slightly with cell passage (>68).

When the holding potential was −50 mV, the current at +10 mV was reduced in amplitude and the slow component of the tail current was absent (Fig. 1 D). This indicates that the SD current was inactivated at this holding potential, but inactivation of the SD current alone cannot account for the amplitude decrease, suggesting that the other component is also subjected to a slower voltage-dependent inactivation.

The current elicited by a depolarizing pulse of 100 ms to +10 mV (maximum current) displayed a relatively fast inactivation and the peak value was considerably bigger than the value at the end of the pulse (Fig. 2). The decaying component represented 40±10% of the total current at this potential and could be approximated by a double exponential function, with $\tau_{h1} = 12 \pm 5$ ms and $\tau_{h2} = 56 \pm 18$ ms (mean ± sd; $n = 21$). Longer (1.5–5 s) depolarizations (not shown) revealed an ultra slow component of inactivation ($\tau_{hs} > 1$ s). This component of the current was not analysed in detail, but the steady-state value of the current at 100 ms was taken as an estimate of this very slowly inactivating component.

To estimate the contribution of the SD current to the total current inactivation, tail currents were measured after depolarizing pulses of increasing duration. The amplitude of the slow component decreased as the depolarization length increased (Fig. 2 B), with a time constant $\tau_{ht} = 15 \pm 3$ ms (mean ± sd; $n = 7$), a value which is close to that of τ_{h1}. This suggested that the constant τ_{h1} was due to inactivation of the SD current.

Inactivation was further studied by a two pulse voltage protocol, which consisted of a test pulse to +10 mV, preceded by a depolarizing prepulse of 50 ms duration and

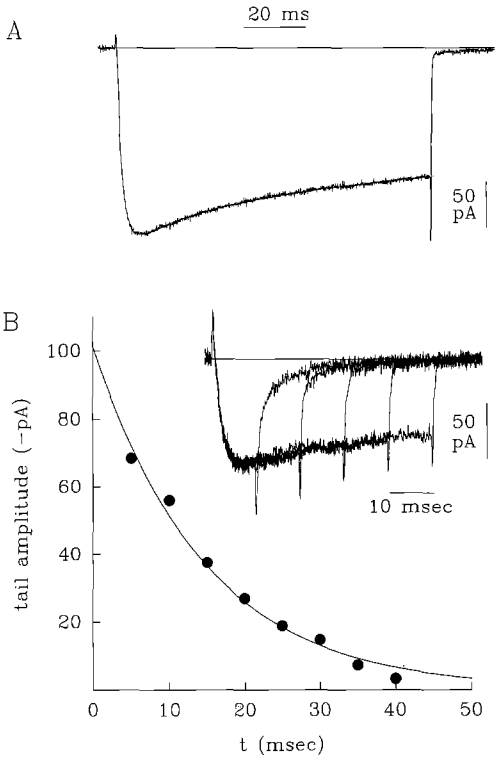

Fig. 2 A, B. Inactivation of the calcium current. **A** The decaying portion of the current trace from −80 to +20 mV was approximated with the function:

$$I(t) = A_1 \exp(-t/\tau_{h1}) + A_2 \exp(-t/\tau_{h2}) + A_3$$

Best fit parameters were:

$\tau_{h1} = 12$ ms; $\tau_{h2} = 63$ ms; $A_1 = -28$ pA; $A_2 = -80$ pA; $A_3 = -110$ pA.

B Dependence of the slow tail current on pulse length. The cell was held at −80 mV and subjected to depolarizations of increasing duration to +10 mV; the repolarization voltage was −50 mV. Tail currents were approximated as in Fig. 1 and the amplitude of the slow component (A_2) was plotted vs. the pulse duration. The experimental points were fitted by a single descending exponential curve. The best fit gave $A = 103$ pA and $\tau = 14.3$ ms

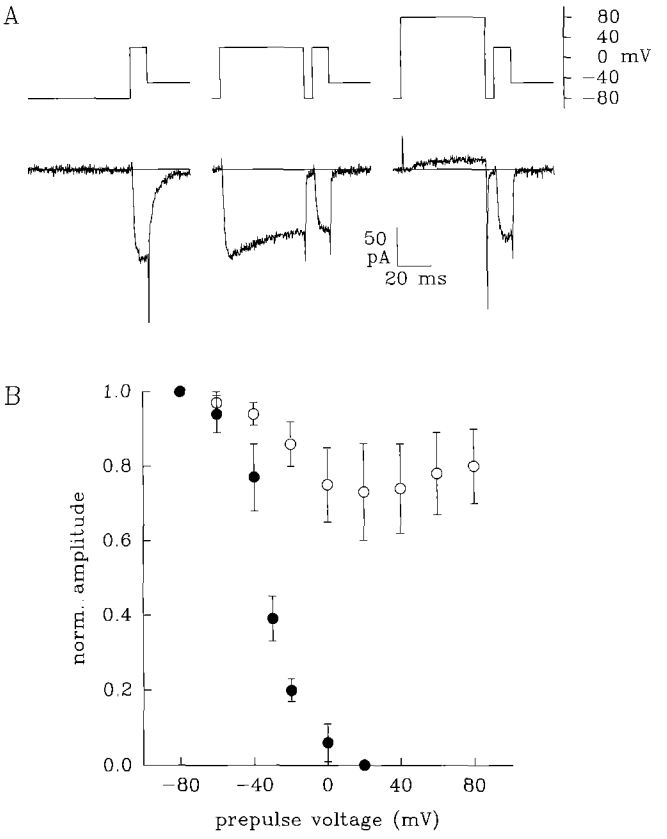

Fig. 3 A, B. Effect of conditioning prepulses on the calcium current and on the tail currents. **A** Current traces from cells subjected to the voltage protocol described in the text and shown above the traces (no prepulse, prepulse to 0 mV and +80 mV). **B** Normalized amplitude of the peak current (o, $n = 12$) and of the slow tail component (●, $n = 8$) vs. the prepulse voltage. Bars represent standard deviations

variable amplitude. The two pulses were separated by a 5 ms return to −80 mV. The depolarizing prepulses caused a decrease of the peak current, which correlated partially with the amplitude of the current elicited by the prepulse (Fig. 3). This effect has been interpreted as a current-dependent inactivation (Plant 1988; Satin and Cook 1989; Hopkins et al. 1991).

In contrast, prepulses to 0 mV or higher completely suppressed the slow component of the tail current and this effect was not correlated with the prepulse current, indicating that it was entirely voltage-dependent.

Similar results were obtained in perforated patch experiments. Repolarization currents clearly contained two components, and the slowly deactivating current was virtually absent when the holding potential was −50 mV, in qualitative agreement with the results obtained in conventional WCR. In this configuration, a virtually undisturbed cytoplasmic environment assures a longer persistence of the calcium current and makes it more feasible to study the calcium-dependent inactivation and the effect of calcium antagonists, such as nifedipine.

The percentage of the current inactivated by the prepulse reached a maximum at 0 mV and it was 33±9% in 10 cells, a percentage which represents ≥80% of the total transient component (Fig. 4). When barium was the charge carrier, the effect was greatly reduced; the moderate decrease of the current for voltage prepulses positive to +20 mV does not correlate with the current amplitude and it is probably due to a minor voltage-dependent inactivation.

The sensitivity to dihydropyridines was tested by two different doses of nifedipine. Nifedipine at 1 μM reduced the maximum calcium current by 22±7% (mean±sd; $n = 10$) and at 10 μM by 38±9% (mean±sd, $n = 19$). The inhibition was almost completely reversible following prolonged wash, but the recovery was strictly dependent on the duration of treatment. The nifedipine-sensitive current activated at high voltage, but reached a peak value at a potential ≈10 mV more negative than the nifedipine-resistant component (Fig. 5).

Nifedipine did not affect the SD current, but only the FD component, as shown by the persistence of the slow

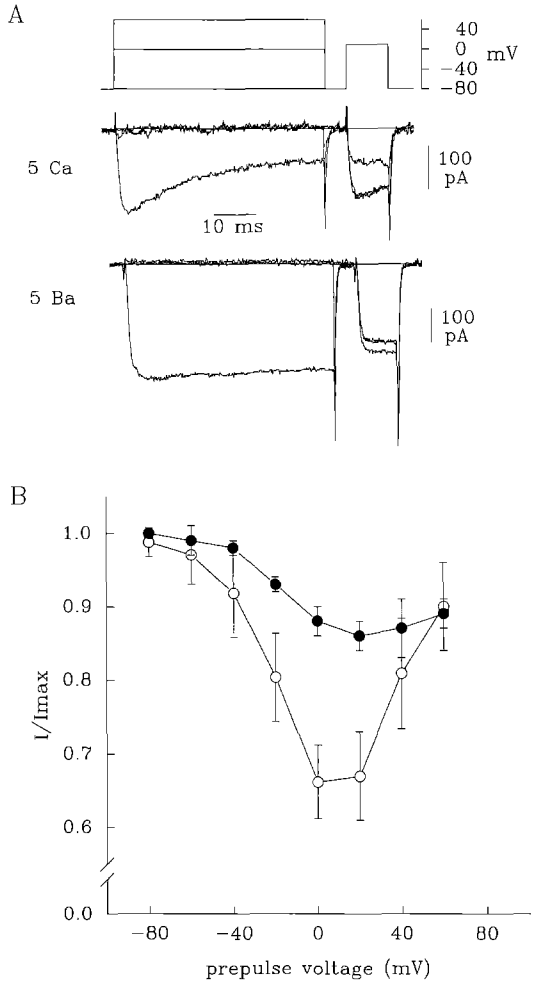

Fig. 4 A, B. Perforated patch recording of whole cell calcium currents. **A** Cells were bathed in either 5 mM Ca or Ba and subjected to the voltage protocol shown above the traces (no prepulse, prepulse to 0 mV and +60 mV, respectively). **B** Normalized amplitude of the peak current in 5 mM Ca (○, $n=15$) and 5 mM Ba (●, $n=4$) vs. prepulse voltage. Bars represent standard deviations

tail current even in the presence of 10 μM nifedipine (Fig. 6). The SD current was nevertheless completely abolished by positive prepulses both in the control and in the presence of the drug.

From inspection of the current traces, it also appears that the nifedipine-sensitive current inactivated more rapidly than the nifedipine-insensitive current (see examples in Figs. 5 to 7). One possible explanation of this effect is that nifedipine affects the decaying and the longer lasting components differently. In 4 cells, nifedipine at 10 μM inhibited the transient portion of the current by $68 \pm 5\%$ and the long lasting (very slowly inactivating) component by $33 \pm 12\%$. This observation suggested that nifedipine preferentially inhibited the calcium-sensitive component and this was confirmed by two pulse experiments (Fig. 7). The nifedipine-resistant current was at most inactivated by $<25\%$ in 4 cells, while the nifedipine-sensitive current was inactivated by 60%.

In contrast to DHPs, ω-conotoxin, fraction GVIA (ω-cgtx; 5–10 μM) did not reduce the HIT calcium currents in 4 cells, despite prolonged (up to 15 min) exposures. This indicates that these cells do not contain this type of Ca channel, at least under these culture conditions.

Discussion

Our results show that the inactivation kinetics of HIT cell calcium current can be described by a relatively fast inactivating component, with double exponential time course ($\tau_{h1} \approx 12$ ms and $\tau_{h2} \approx 60$ ms) and a very slowly inactivating component ($\tau > 1$ s). These three components can be correlated with three currents with different kinetic and pharmacological properties. We summarize these properties and compare our observations with previous findings.

The faster component (τ_{h1}) is primarily due to the inactivation of a low-voltage-activated current, which is best

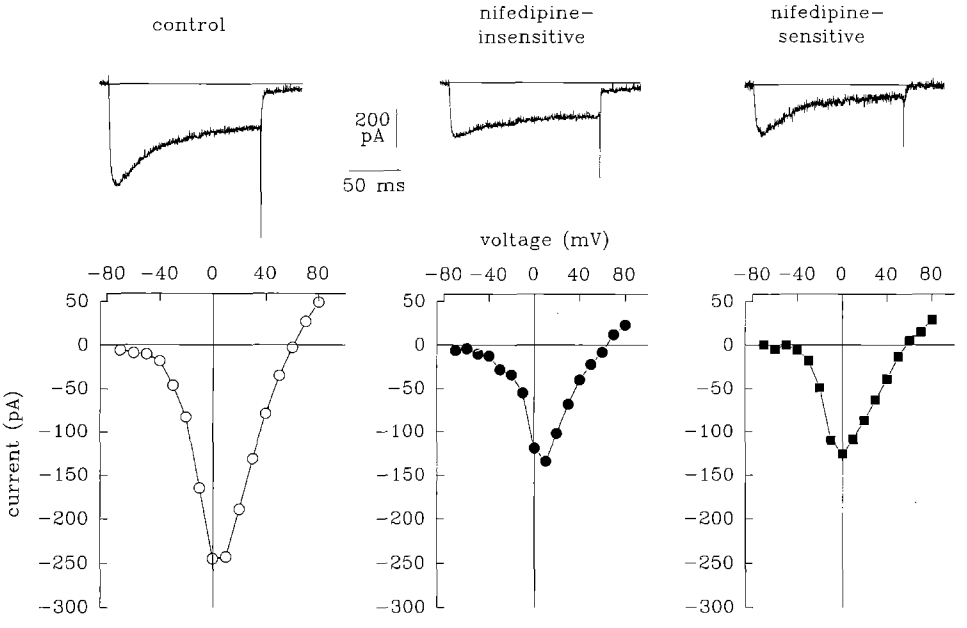

Fig. 5. Effect of nifedipine on the calcium current in perforated patch configuration. Traces represent the current at +10 mV in control (*left*), in the presence of 10 μM nifedipine (*middle*) and the nifedipine-sensitive current, obtained by digital subtraction (*right*). The holding potential was −80 mV. Graphs are corresponding current-voltage relationships

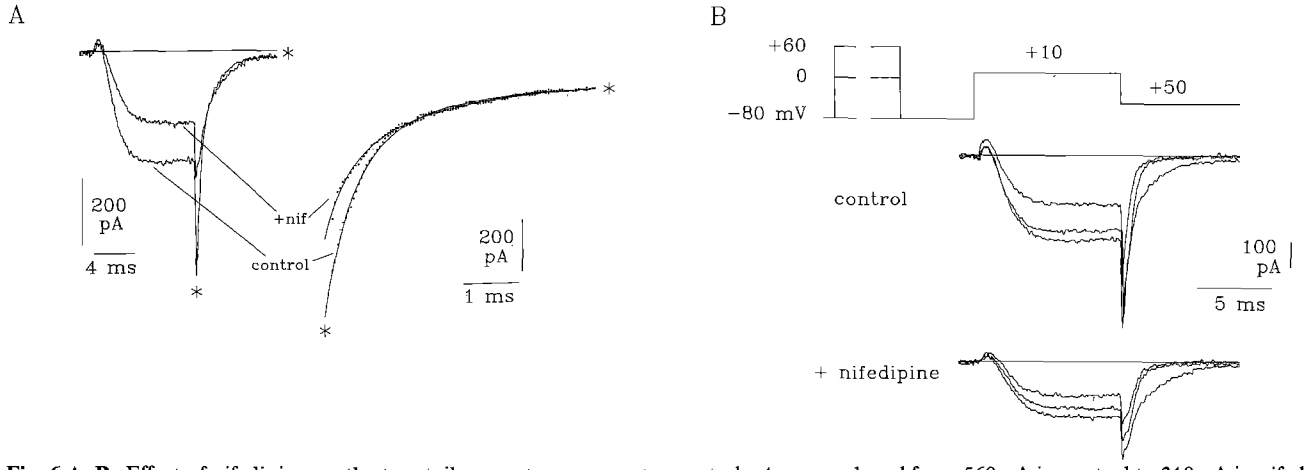

Fig. 6 A, B. Effect of nifedipine on the two tail current components in perforated patch configuration. **A** Current traces at +10 mV in control and in the presence of 10 μM nifedipine. Current were sampled at 50 μs/point. Tail currents are expanded on the right and were approximated as in Fig. 2. The first 400 μs were blanked and exponential functions were extrapolated to 0. Note that the evaluation of time constants is not accurate in this conditions, but the best fit gave $\tau_1 = 0.45$ ms and $\tau_2 = 2$ ms in both conditions. The amplitude A_1 was reduced from 560 pA in control to 310 pA in nifedipine, while A_2 was not modified and the two tail traces overlap for $t > 1$ ms after repolarization. **B** Effect of the prepulse on tail currents in the control and in the presence of nifedipine. Cells were subjected to the same voltage protocol as in Figs. 5 and 6. The traces shown are relative to the following prepulse values: −80 mV (no prepulse), 0 mV and +60 mV. The prepulses eliminate the slow component of the tail current

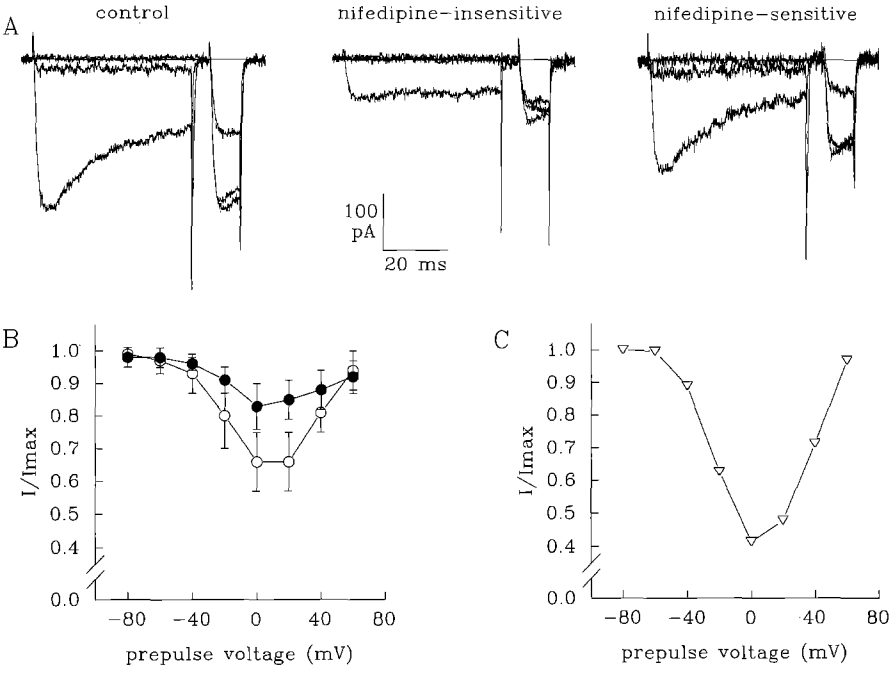

Fig. 7. Effect of the prepulse on perforated patch whole cell current in control and in the presence of nifedipine. **A** Current traces in control (*left*) and in the presence of nifedipine (*middle*) and traces obtained by digital subtraction of the nifedipine-resistant current from the control current (*right*). **B** The normalized amplitude of the peak current vs. prepulse voltage in the presence of nifedipine (●, $n = 4$) is compared with the control values (○, $n = 15$). Bars represent standard deviations. **C** Normalized amplitude of the peak nifedipine-sensitive currents vs. prepulse voltage in the same cell as the above traces. This current was maximally inactivated by 60%, while the nifedipine-resistant current showed a maximum inactivation of 22% in this cell

resolved by tail current measurements and represents a small ($\leq 25\%$) percentage of the total current. This component inactivates entirely through voltage, is not sensitive to DHPs and is similar in all respects to the neuronal T-type current (reviewed in Carbone and Swandulla (1989)), already reported in rat β-cells (Hiriart and Matteson 1988; Satin and Cook 1988) and HIT cells (Satin and Cook 1988).

The second component (τ_{h2}) is due to a high-voltage-activated current, which inactivates primarily through current driven calcium influx, as indicated by the fact that the percentage of current inactivation is correlated with the amplitude of the current activated by a preceding pulse and is drastically reduced when barium is the charge carrier. This component is inhibited by $\approx 70\%$ by nifedipine. Preliminary data also indicate that this component is the main target of the agonist dihydropyridine BayK 8644, which increased the transient portion of the current, enhanced the percentage of current-dependent inactivation, and shifted the activation curve in the negative direction (Marchetti et al. 1993 and *unpublished observations*). Calcium-dependent inactivation is a well known property of DHP-sensitive calcium currents (Eckert and Chad 1984; Kalman et al. 1988). This current is similar to the fast ($\tau_h \approx 60-70$ ms) calcium-dependent inactivating and DHP-sensitive current described in prima-

ry rat (Satin and Cook 1989), mouse (Hopkins et al. 1991), dog (Pressler and Misler 1991) and human (Kelly et al. 1991) β-cells, but it is different from the L-type current described in DRG neurons (Fox et al. 1987), which inactivates slowly and through a voltage-dependent mechanism.

The third, very slowly inactivated component, is also activated at high voltage, but is less subject to calcium-dependent inactivation and is more weakly sensitive to DHP. A similar current has been described in HIT cells (Satin and Cook 1989) and mouse β-cells (Cook et al. 1991; Hopkins et al. 1991). Its slow voltage-dependent inactivation might be responsible for the decrease in the amplitude of the current produced by a holding potential of −50 mV (Fig. 1; Satin and Cook 1989; Kelly et al. 1991).

An important finding of this study is that a large portion of the calcium current of HIT cells is insensitive to the DHP antagonist nifedipine, even at a dose which we estimate to be saturating. In partial agreement, preliminary data on single channels in cell-attached patches from these cells suggested the presence of DHP-insensitive barium channels (Marchetti 1993).

The existence of a sizeable portion of DHP-insensitive current has been detailed for the first time in RINm5F and human β-cells by Pollo et al. (1993). Their results, and ours, are in partial agreement with previous observations of an incomplete block of calcium current in primary β-cells (Satin and Cook 1988; Hopkins et al. 1991). However, our results are in conflict with earlier work on HIT cells which showed nearly 80% block of the current by nimodipine (Keahey et al. 1989). These authors also failed to identify a low-threshold DHP-insensitive current, which is frequently present in this β-cells line (Satin and Cook 1988). This is an indication of a possible discrepancy in the culture conditions.

Contrary to the original classification by Fox et al. (1987) which described the DHP-insensitive current as fast inactivating ('N-type' current), a slowly inactivating DHP-insensitive current with similar properties has been identified in neurons (Aosaki and Kasai 1988; Kasai and Neher 1992), chromaffin cells (Artalejo et al. 1992) and RINm5F (Pollo et al. 1993).

Despite their pharmacological diversity, the inactivating and non-inactivating high-voltage-activated currents have similar permeability properties and conduct barium better than calcium (Carbone et al. 1990; Kasai and Neher 1992; Pollo et al. 1993). In our experiments, the deactivation kinetics of the two currents were also rather indistinguishible, an indication that would argue in favour of a single type of high-voltage-activated channel (Swandulla and Armstrong 1988; Hiriart and Matteson 1988). Other authors have reported small differences in tail current kinetics (Kasai and Neher 1992; Pollo et al. 1993), but in general, tail current kinetics do not seem a very appropriate tool for separating the different components of the high-voltage-activated current (Regan et al. 1991). From the current/voltage relationship, the nifedipine-sensitive current appeared to activate slightly more negative than the nifedipine-resistant current, in agreement with previous observations in neurons (Kasai and Neher 1992) and RINm5F cells (Pollo et al. 1993).

However, in contrast with neuronal (Kasai and Neher 1992) and RINm5F cells (Aicardi et al. 1991; Sher et al. 1992), we were unable to assign a pharmacological identity to the slowly inactivating nifedipine-resistant portion of the current, because the ω-cgtx had no effect in these cells, just as it did not affect the calcium current of human β-cells (Pollo et al. 1993). As pointed out by these authors, the presence of ω-cgtx-sensitive channels may be linked to the culture conditions and the ω-cgtx-sensitive current developed in RINm5F cells after the outgrowth of neuronal-like processes, which are never seen in HIT cultures in our conditions. DHP- and ω-cgtx-insensitive calcium channels have been reported in various neuronal preparations and seem to be present in small number also in RINmF5 and human β-cells (Pollo et al. 1993). Some of these channels are blocked by different toxins, including ω-agatoxin-IVA ('P-type' channel: Regan et al. 1991; Mintz et al. 1992) and ω-conotoxin-MVIIC (Hilliard et al. 1992). However, it is clear that the kinetic characterization alone is not sufficient to ascribe the DHP-insensitive current of HIT in any of these classes.

Our description suggests that three calcium currents would be involved in the generation of electrical activity in insulin-secreting cells. The T-type (or SD) current may play a role in the onset of burst and provide a positive feedback to open high-voltage-activated channels. A similar role is played by sodium channels in certain β-cells types, which lack T-type calcium channels (Pressler and Misler 1991). HIT cells deprived of this component might be unable to start the typical electrical activity which triggers calcium rise and secretion, as suggested by the progressive decrease of SD current in cells from higher passages, which are known to secrete much less in response to glucose.

The activity during burst is primarily sustained by the DHP-sensitive current, which has a slightly lower threshold than the DHP-resistant slow current and is inactivated by calcium entry, thus contributing to single spike repolarization. The primary role in the control of calcium entry and secretion of the DHP-sensitive current is confirmed by the observation that DHP antagonists significantly inhibit insulin secretion and cause hyperglycemia (see Ashcroft and Rorsman 1989). Preliminary measurements of internal calcium with the fluorescent probe Fura2 showed that 1 μM nimodipine (another DHP antagonist) almost completely abolished the rise in internal calcium induced by suprathreshold glucose in HIT cells (C. Marchetti and C. Usai unpublished data).

Finally, the very slow voltage-dependent inactivation of a portion of high-voltage-activated current has been proposed to be the main cause of burst termination (Cook et al. 1991; Hopkins et al. 1991; Pressler and Misler 1991). Note that calcium-dependent inactivation is unlikely to play a role in this respect because it occurs in a different (faster) time scale.

References

Aicardi G, Pollo A, Sher E, Carbone E (1991) Noradrenergic inhibition and voltage-dependent facilitation of ω-conotoxin-sensitive Ca channels in insuline-secreting Rinm5F cells. FEBS Lett 281:201–204

Aosaki T, Kasai H (1989) Characterization of two kinds of high-voltage-activated Ca-current in chick sensory neurons. Pflügers Arch 414:150–156

Artalejo CR, Perlman RL, Fox AP (1992) Ω-conotoxin GVIA blocks a Ca^{2+} current in bovine chromaffin cells that is not of the "classic" N type. Neuron 8:85–95

Ashcroft FM, Rorsman P (1989) Electrophysiology of pancreatic β-cells. Prog Biophys Mol Biol 54:87–143

Ashcroft FM, Kelly RP, Smith PA (1990) Two types of Ca channel in rat pancreatic β-cells. Pflügers Arch 415:504–506

Carbone E, Swandulla D (1989) Neuronal calcium channels: kinetics, blockade and modulation. Prog Biophys Mol Biol 54: 31–58

Carbone E, Sher E, Clementi F (1990) Ca currents in human neuroblastoma IMR32 cells: kinetics, permeability and pharmacology. Pflügers Arch 416:170–179

Cook DL, Satin LS, Hopkins WF (1991) Pancreatic B cells are bursting, but how? TINS 14:411–414

Cota G (1986) Calcium channel currents in pars intermedia cells of the rat pituitary gland. J Gen Physiol 88:83–105

Eckert R, Chad JE (1984) Inactivation of calcium channels. Prog Biophys Mol Biol 44:215–267

Fox AP, Nowycky MC, Tsien RW (1987) Kinetic and pharmacological properties distinguishing three types of calcium currents in chick sensory neurons. J Physiol 394:149–172

Hamill OP, Marty A, Neher E, Sakman B, Sigworth FJ (1981) Improved patch clamp techniques for high resolution current recording from cells and cell-free membrane patches. Pflügers Arch 391:85–100

Hilliard DR, Monje VD, Mintz IM, Bean BP, Nadasdi L, Ramachandran J, Miljanich G, Azimi-Zoonooz A, McIntosh JM, Cruz LJ, Imperial JS, Olivera BM (1992) A new conus peptide ligand for mammalian presynaptic Ca^{2+} channels. Neuron 9: 69–77

Hiriart M, Matteson DR (1988) Na channels and two types of Ca channels in rat pancreatic B cells identified with the reverse hemolytic plaque assay. J Gen Physiol 91:617–639

Hopkins WF, Satins LS, Cook DL (1991) Inactivation kinetics and pharmacology distinguish two calcium currents in mouse pancreatic B-cells. J Membr Biol 119:229–239

Horn R, Marty A (1988) Muscarinic activation of ionic currents measured by a new whole-cell recording method. J Gen Physiol 92:145–159

Hsu WH, Xiang H, Rajan AS, Kunze DL (1991) Somatostatin inhibits insulin secretion by a G-protein-mediated decrease in Ca^{2+} entry through voltage-dependent Ca^{2+} channels in beta cell. J Biol Chem 266:837–843

Kalman D, O'Lague PH, Erxleben C, Armstrong DL (1988) Calcium-dependent inactivation of the dihydropyridine-sensitive calcium channels in GH_3 cells. J Gen Physiol 92:531–548

Kasai H, Neher E (1992) Dihydropyridine-sensitive and ω-conotoxin-sensitive channels in a mammalian neuroblastoma-glioma cell line. J Physiol 448:161–188

Keahey HH, Rajan AS, Boyd AE III (1989) Characterization of voltage-dependent calcium channels in a β-cell line. Diabetes 38:188–193

Keizer J, Smolen P (1991) Bursting electrical activity in pancreatic β cells caused by Ca^{2+}- and voltage-inactivated Ca^{2+} channels. Proc Natl Acad Sci, USA 88:3897–3901

Kelly RP, Sutton R, Ashcroft FM (1991) Voltage-activated calcium and potassium currents in human pancreatic β-cells. J Physiol 443:175–192

Korn SJ, Horn R (1989) Influence of sodium-calcium exchange on calcium current rundown and the duration of calcium-dependent chloride current in pituitary cells, studied with whole cell and perforated patch recording. J Gen Physiol 94:789–812

Marchetti C (1993) Voltage-dependent calcium channels in insuline-secreting cells. Proceeding of the VII AIFB Congress. Phys Medica IX (Suppl. 1): 9–11

Marchetti C, Amico C, Robello M (1993) The patch-recording technique: different approaches in a clonal pancreatic B-cell line. Phys Medica, IX (4) (in press)

Matteson DR, Armstrong CM (1986) Properties of two types of calcium channels in clonal pituitary cells. J Gen Physiol 87: 161–182

Mintz IM, Adams ME, Bean BP (1992) P-type calcium channels in rat central and peripheral neurons. Neuron 9:85–95

Parsey RV, Matteson DR (1993) Ascorbic acid modulation of calcium channels in pancreatic β cells. J Gen Physiol 102:503–523

Plant TD (1988) Properties and calcium-dependent inactivation of calcium currents in cultured mouse pancreatic β-cells. J Physiol 404:731–747

Pressler DM, Misler S (1991) Role of voltage-dependent ionic currents in coupling glucose stimulation to insuline secretion in canine pancreatic islet B-cells. J Membr Biol 124:239–253

Pollo A, Lovatto M, Biancardi E, Sher E, Socci C, Carbone E (1993) Sensitivity to dihydropyridines, ω-conotoxin and noradrenaline reveals HVA channels in rat insulinoma and human pancreatic β-cells. Pflügers Arch 423:462–471

Regan LJ, Sah DWY, Bean BP (1991) Ca^{2+} channels in rat central and peripheral neurons: high-threshold current resistant to dihydropyridine blockers and ω-conotoxin. Neuron 6:269–280

Rorsman P, Trube G (1986) Calcium and delayed potassium currents in mouse pancreatic β-cells under voltage-clamp conditions. J Physiol 374:531–550

Rorsman P, Ashcroft FM, Trube G (1988) Single Ca channel currents in mouse pancreatic B-cells. Pflügers Arch 412:597–603

Sala S, Matteson DR (1990) Single-channel recording of two types of calcium channels in rat pancreatic β-cells. Biophys J 58:567–571

Sala S, Parsey RV, Cohen AS, Matteson DR (1991) Analysis and use of perforated patch technique for recording ionic currents in pancreatic β-cells. J Membr Biol 122:177–187

Santerre RF, Cook RA, Crisel RMD, Sharp JD, Schmidt RJ, Williams DC, Wilson CP (1981) Insulin synthesis in a clonal cell line of simian virus 40-transformed hamster pancreatic beta cells. Proc Natl Acad Sci, USA 78:4339–4343

Satin LS, Cook DL (1988) Evidence for two calcium currents in insuline-secreting cells. Pflügers Arch 411:401–409

Satin LS, Cook DL (1989) Calcium current inactivation in insuline-secreting cells is mediated by calcium influx and membrane depolarization. Pflügers Arch 414:1–10

Sher E, Biancardi E, Pollo A, Carbone E, Li G, Wollheim CB, Clementi F (1992) Ω-conotoxin-sensitive, voltage operated Ca^{2+} channels in insulin-secreting cells. Eur J Pharmacol 216:407–414

Smolen P, Keizer J (1992) Slow voltage inactivation of Ca^{2+} currents and bursting mechanism for the mouse pancreatic beta-cell. J Membr Biol 127:9–19

Swandulla D, Armstrong CM (1988) Fast-deactiving calcium channels in chick sensory neurons. J Gen Physiol 92:197–218

Swandulla D, Carbone E, Lux HD (1991) Do calcium channel classifications account for neuronal calcium channel diversity? TINS 14:46–51